DINAME 2023 - Proceedings of the XIX International Symposium on Dynamic Problems of Mechanics,
A.S. De Paula, A.T. Fabro and M.R. Machado (Editors), ABCM.
Pirenópolis, Go, Brazil, February 26th to March 3rd, 2023

Reduction of Negative Damping Effects in the Drilling Process Using Active Control

Hélio Jacinto da Cruz Neto[1], **Marcelo Areias Trindade**[1]

[1] São Carlos School of Engineering - University of São Paulo, Department of Mechanical Engineering, Av. Trabalhador São Carlense, 400, São Carlos, SP, 13566-590, Brazil

Abstract: Failures during oil extraction can have impacts on exploration costs and time, especially those caused by vibrations during the drilling phase. A proper way to reduce these detrimental failures is to design an active controller that efficiently mitigates vibrations with the constraint of using the limited amount of data available in field operations. This paper proposes a novel control technique that uses linear combinations of measured signals and aims to counterbalance negative damping effects. The proposed controller is applied to a representative drill string model, modeled using the finite element method with non-regularized dry friction. The particular aspects regarding the application of the proposed controller for the drill string problem, i.e., reformulation of the equations of motion as a stabilization problem, determination of the output matrix, and linearization are addressed. Simulations indicate that the proposed controller presents remarkable robustness regarding parameter variations, while still maintaining good nominal performance.

Keywords: drill string vibrations, stick-slip, negative damping, output feedback, active control

INTRODUCTION

Vibrations are one of the main factors for drill string failure, yielding delays and increased costs in oil production (Jardine *et al.*, 1994; Dong and Chen, 2016), and consequently drawing great interest for the oil and gas industry to mitigate them. Several approaches have been proposed to model and control drill string torsional vibrations, most relying on active control techniques (Zhu *et al.*, 2014). Although strategies that deviate from the standard PI control can provide a better performance, they are often based on assumptions that may not be feasible on typical drilling rigs. A few examples are controllers that require measurement of all system states (Vaziri *et al.*, 2020) estimation of unmeasured states using dynamic observers (Vromen *et al.*, 2017) - that may produce time delay, lower stability margins and spillover - and no modeling errors (Abdulgalil and Siguerdidjane, 2004). The design of an effective controller with a wide range of applications in a variety of oil wells must consider not only performance but all the aforementioned constraints.

Recognizing these constraints and the high variability involved in the drilling process, this work proposes a simple control law, based only on static output feedback, with the objective of allowing the closed-loop system to tolerate large variations in unknown parameters. The proposed control strategy is based on the physical characteristics of the drilling process, and aims to counterbalance negative damping effects generated at the drill bit. The results indicate that the proposed controller presents remarkable robustness regarding parameter variations, while still maintaining good nominal performance, and that the linear system can provide reliable information about the global stability of the operating point.

DRILL STRING TORSIONAL DYNAMICS MODEL

The torsional dynamics of the drilling system is represented in a simplified way considering three main components: the rotary table, the bottom hole assembly (BHA) and the drill string, which are depicted schematically in Fig. 1. The BHA contains the stabilizers, drill-collars and drill-bit and, for modeling purposes, is represented as a rigid body, same hypothesis assumed for the rotary table. The drill string is modeled as a circular shaft using the fundamental torsional-deformation assumptions and the material is considered linear elastic with constant properties, which are given in Tab. 1.

Table 1 – Numerical values of the drilling system general parameters.

Drill string mass density (kg/m^3)	8010
Drill string shear modulus (GPa)	79.6
Drill string length (m)	3000
Drill string inner radius - R_i (m)	0.0543
Drill string outer radius - R_o (m)	0.0635
BHA effective rotary inertia ($kg.m^2$)	394
Driving table effective rotary inertia ($kg.m^2$)	500

Two main external sources are acting on this system: a drive torque on the rotary table and a reaction torque induced by the bit-rock interaction. The drive torque is taken as a control input variable, which will be determined in the controller

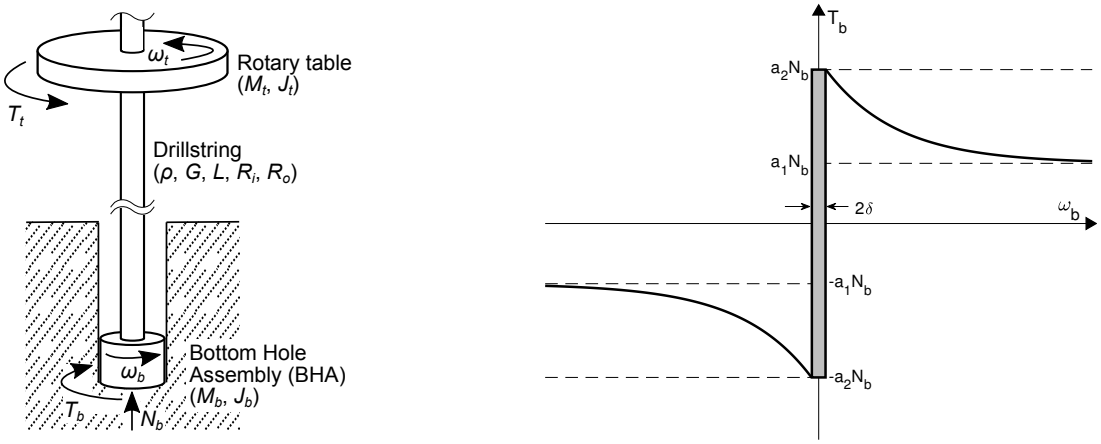

Figure 1 – Components of the rotary drilling system (left) and reaction torque as a function of the angular velocity (right).

design section. The reaction torque is modeled as frictional force using Karnopp's model with an exponential decaying friction term (Fig. 1), with $N_b = WOB$:

$$T_b = \begin{cases} T, & \text{for } |\omega_b| \leq \delta \text{ and } |T| \leq a_2 WOB, \\ a_2 WOB sgn(T), & \text{for } |\omega_b| \leq \delta \text{ and } |T| > a_2 WOB, \\ \left[a_1 + (a_2 - a_1)e^{-\beta|\omega_b|}\right] WOB sgn(\omega_b), & \text{for } |\omega_b| > \delta. \end{cases} \tag{1}$$

in which T is the torque applied to the bit by the drill string, N_b is the normal force applied by the rock formation to the bit, the values a_2 and a_1 are the static and dynamic friction coefficients, respectively, β is a positive exponential friction coefficient, ω_b is the bit angular speed and the width of the region of stick phase is set to $\delta = 10^{-4}$ rad/s. An experimental identification of the friction parameters was conducted by Tucker and Wang (2003) for WOB values around 100 kN and target speeds around 100 rpm. Based on that identification, Tucker and Wang (2003) developed a regularized friction model using correlations between torque-on-bit, bit rotary speed and WOB to extend the analysis for other operating conditions. Since a regularized model may misrepresent the stick phase, Monteiro and Trindade (2017) adapted those correlations to a more realistic non-regularized dry friction model. The friction parameters values obtained by Monteiro and Trindade (2017) are given in Tab. 2 as a function of the WOB.

Table 2 – Dry friction parameters for different values of WOB.

WOB (kN)	80	100	120	140	160
a_1 (m)	0.037	0.032	0.029	0.026	0.025
a_2 (m)	0.057	0.070	0.079	0.085	0.089
β $(s.rad^{-1})$	0.082	0.093	0.097	0.098	0.099

A FE model with a regular mesh using 30 elements was constructed to represent the drill string. The regular mesh was refined until convergence was achieved for the natural frequencies up to 6 Hz. Hermite cubics were adopted as interpolation functions to improve convergence. A modal reduction was proposed to reduce computational cost, keeping only the thirteen modes that were in the 0 to 6 Hz frequency range (including one rigid body mode). The approximate eigenfunctions were determined to allow sensors positioning along the drill string in the controller design. Finally, to represent the general dissipation sources, a modal damping factor of 1% was added for each mode. Given these assumptions, the system equations in modal coordinates are

$$\ddot{\boldsymbol{\eta}} + \mathbf{D}\dot{\boldsymbol{\eta}} + \boldsymbol{\Lambda}\boldsymbol{\eta} = \boldsymbol{\phi}(0)T_t - \boldsymbol{\phi}(L)T_b, \tag{2}$$

in which $\boldsymbol{\eta} \in \mathbb{R}^n$ is the vector of modal displacements, $\boldsymbol{\Lambda} \in \mathbb{R}^{n\times n}$ is a diagonal matrix of system eigenvalues or natural frequencies squared, $\mathbf{D} \in \mathbb{R}^{n\times n}$ is a diagonal matrix of damping and $\boldsymbol{\phi}\colon \mathbb{R} \to \mathbb{R}^n$ represents the approximated eigenfunctions. Note that since the natural frequency associated with the rigid body mode is null, neither the rigid body displacement nor its derivative appears in Eq. (2). Thus, when transforming Eq. (2) to differential equations of first order – for controller design, dynamic analysis and numerical integration – it is not necessary to define the rigid body displacement as a state. These observations motivate the definition of a state without the rigid body displacement

$$\mathbf{x} = \begin{bmatrix} \eta_2 & \dots & \eta_n & \dot{\eta}_1 & \dots & \dot{\eta}_n \end{bmatrix}^\intercal = \begin{bmatrix} \bar{\boldsymbol{\eta}}^\intercal & \dot{\boldsymbol{\eta}}^\intercal \end{bmatrix}^\intercal, \tag{3}$$

which leads to the following equations of motion using a state space representation:

$$\begin{aligned}&\dot{\mathbf{x}} = \mathbf{A}\mathbf{x} + \mathbf{B}_c T_t + \mathbf{B}_r T_b = \mathbf{f}(\mathbf{x}, T_t)\\ &\mathbf{A} = \begin{bmatrix} \mathbf{0} & \bar{\mathbf{I}} \\ -\bar{\mathbf{\Lambda}} & -\mathbf{D} \end{bmatrix}, \quad \mathbf{B}_c = \begin{bmatrix} \mathbf{0} \\ \boldsymbol{\phi}(0) \end{bmatrix}, \quad \mathbf{B}_r = \begin{bmatrix} \mathbf{0} \\ -\boldsymbol{\phi}(L) \end{bmatrix}.\end{aligned} \tag{4}$$

In Eqs. (3) and (4), a bar over a letter is used to distinguish between variables with and without components associated with the rigid body mode, i.e., $\bar{\mathbf{\Lambda}}$ is the matrix $\mathbf{\Lambda}$ without the first column, $\bar{\boldsymbol{I}}$ is the identity matrix without the first row and $\bar{\boldsymbol{\eta}}$ is the vector $\boldsymbol{\eta}$ without the first element.

Model Reformulation for Controller Design

Some of the analyses developed in the following sections are more conveniently done if the operating point is at the origin of the coordinate system. Since the desired operating configuration is characterized by the entire drill string rotating deformed with a constant velocity, its representation using the state defined in Eq. (3) is already constant, but not zero (with the rigid body displacement, the desired state would be a function of time, and a further step would be necessary to remove it). Thus, the first steps in reformulating the system equations aim to shift the operating point to the origin of a new coordinate system. For that, let the configuration corresponding to the drill string rotating at the desired angular velocity (ω_r) in terms of system states be

$$\mathbf{x}_{eq} = \begin{bmatrix} \bar{\boldsymbol{\eta}}_{eq} \\ \dot{\bar{\boldsymbol{\eta}}}_{eq} \end{bmatrix}. \tag{5}$$

Then, the applied control torque T_t is decomposed into a feedback component u, to suppress vibrations, and a constant feedforward component $\tilde{u}$, inducing $\mathbf{x}_{eq}$, such that

$$T_t = \tilde{u} + u. \tag{6}$$

The constant parameters $\mathbf{x}_{eq}$ and $\tilde{u}$ are given by the relation $\omega_r = \boldsymbol{\phi}^\intercal(L)\dot{\boldsymbol{\eta}}_{eq}$ combined with the equilibrium condition of Eq. (4), $\mathbf{f}(\mathbf{x}_{eq}, \tilde{u}) = \mathbf{0}$:

$$\mathbf{A}\mathbf{x}_{eq} + \mathbf{B}_t\tilde{u} + \mathbf{B}_b T_b(\omega_r) = \mathbf{0}. \tag{7}$$

Next, define the new coordinate system $\boldsymbol{\xi}$ by the translation:

$$\boldsymbol{\xi} = \begin{bmatrix} \boldsymbol{\xi}_d \\ \boldsymbol{\xi}_v \end{bmatrix} = \begin{bmatrix} \bar{\boldsymbol{\eta}} - \bar{\boldsymbol{\eta}}_{eq} \\ \dot{\bar{\boldsymbol{\eta}}} - \dot{\bar{\boldsymbol{\eta}}}_{eq} \end{bmatrix} = \mathbf{x} - \mathbf{x}_{eq}. \tag{8}$$

Finally, the substitution of Eqs. (6) and (8) into Eq. (4) leads to the equations of motion in coordinate $\boldsymbol{\xi}$

$$\dot{\boldsymbol{\xi}} = \mathbf{A}\boldsymbol{\xi} + \mathbf{B}_t u + \mathbf{B}_b q(\omega_d) = \mathbf{g}(\boldsymbol{\xi}, u), \tag{9}$$

in which the desired operating point has been shifted to the origin. In Eq. (9), $q(\omega_d)$ is a translated reaction torque

$$q(\omega_d) = T_b(\omega_d + \omega_r) - T_b(\omega_r) = T_b\left(\boldsymbol{\phi}^\intercal(L)\boldsymbol{\xi}_v + \omega_r\right) - T_b(\omega_r), \tag{10}$$

such that $q(0) = 0$, and ω_d is the difference between the drill bit and target velocities

$$\omega_d = \omega_b - \omega_r = \boldsymbol{\phi}^\intercal(L)\boldsymbol{\xi}_v. \tag{11}$$

Equation (9) was obtained on the assumption that Eq. (7) holds, and consequently, $\tilde{u} = T_b(\omega_r)$. However, as the bit-rock interaction variables are rarely know and subject to changes according to the drill bit condition and the rock formation lithology, there is the possibility that $\tilde{u} \neq T_b(\omega_r)$, and the feedforward torque $\tilde{u}$ may yield a steady-state error. To ensure that at the equilibrium the drill string rotates with the desired angular velocity, Eq. (9) is augmented with the error integral

$$\dot{\sigma} = e = \omega_t - \omega_r = \boldsymbol{\phi}^\intercal(0)\boldsymbol{\xi}_v \tag{12}$$

yielding the augmented system

$$\dot{\boldsymbol{\zeta}} = \begin{bmatrix} \dot{\sigma} \\ \dot{\boldsymbol{\xi}} \end{bmatrix} = \begin{bmatrix} \boldsymbol{\phi}^\intercal(0)\boldsymbol{\xi}_v \\ \mathbf{A}\boldsymbol{\xi} + \mathbf{B}_t u + \mathbf{B}_b q(\omega_d) \end{bmatrix} = \mathbf{A}_n\boldsymbol{\zeta} + \mathbf{B}_{tn}u + \mathbf{B}_{bn}q(\omega_d) = \mathbf{h}(\boldsymbol{\zeta}, u). \tag{13}$$

At first, it may seem artificial to augment the system with the error integral since the dynamics of $\boldsymbol{\xi}$ do not depend on σ. However, the idea of adding σ as a state is to measure this variable and use it for feedback, such that u, and consequently $\boldsymbol{\xi}$, become a function of σ. This is a standard procedure in control theory known as integral action that guarantees regulation in the presence of uncertainties if the closed-loop system is structurally stable (Khalil, 2002).

OPEN-LOOP ANALYSIS

This section investigates the stability of the operating point considering the open-loop system described by Eq. (9). For a target angular velocity ω_r sufficiently greater than zero, q is a smooth function of ω_d, and the qualitative behavior of the solutions of equation (9) in a neighborhood of the origin can be determined by a linear approximation at this point (assuming $\boldsymbol{\xi} = \mathbf{0}$ is hyperbolic). Linearization of Eq. (9) at the origin leads to the associated linear system

$$\mathbf{z} = \mathbf{A}_l \mathbf{z}, \tag{14}$$

in which $\mathbf{A}_l$ is the matrix of first order partial derivatives of $\mathbf{g}$ with respect to $\boldsymbol{\xi}$, evaluated at the origin

$$\mathbf{A}_l = \left.\frac{\partial \mathbf{g}}{\partial \boldsymbol{\xi}}\right|_{\boldsymbol{\xi}=\mathbf{0}} = \begin{bmatrix} \mathbf{0} & \bar{\mathbf{I}} \\ -\bar{\mathbf{\Lambda}} & -[\mathbf{D} + n_d \boldsymbol{\phi}(L)\boldsymbol{\phi}^\intercal(L)] \end{bmatrix}, \tag{15}$$

where n_d is the derivative of q at zero

$$n_d = \left.\frac{\mathrm{d}q}{\mathrm{d}\omega_d}\right|_{\omega_d=0} = -\beta(a_2 - a_1)e^{-\beta\omega_r} WOB. \tag{16}$$

Matrix $\mathbf{A}_l$, which represents the linearized system dynamics, is a combination of matrix $\mathbf{A}$, which characterizes the dynamics of the drill string itself, and matrix $n_d\boldsymbol{\phi}(L)\boldsymbol{\phi}^\intercal(L)$, which is the local contribution of the bit-rock interaction. This contribution appears in matrix $\mathbf{A}_l$ together with the term $\mathbf{D}$, which represents system dissipation factors. However, as the matrix $\boldsymbol{\phi}(L)\boldsymbol{\phi}^\intercal(L)$ is positive semi-definite and the coefficient n_d is negative, this contribution produces the opposite effect of the energy dissipation term $\mathbf{D}$. Thus, the reaction torque applied to the bit is locally equivalent to a viscous damper with a negative damping coefficient n_d, yielding the observed instability in field operations.

The apparent negative damping effect has already been described in classical nonlinear oscillations texts and is regarded as a source of instability of equilibrium points and the existence of limit cycles, see for example the Van der Pol oscillator and Froude's pendulum (Andronov *et al.*, 1966; Guckenheimer and Holmes, 1983). Several works (Brett, 1992; Mihajlović *et al.*, 2004; Saldivar *et al.*, 2013) also mention negative damping as one of the causes of instability and occurrence of stick-slip oscillations for the drilling problem in oil wells. The expression derived in Eq. (16) based on the friction model adopted in Eq. (1) not only corroborates these statements, but introduces the concept of the negative damping coefficient based on the linear approximation and indicates how the drilling parameters affect its magnitude. Therefore, field observations (Brett, 1992) indicating that increasing the WOB or decreasing the angular velocity may lead to unstable drilling operations can be explained using the negative damping coefficient, since both of the described operations increase its magnitude. Likewise, higher values of the difference between static and dynamic friction coefficients produce the same effect on n_d and can also induce instability. Such direct relationships cannot be drawn for the decay rate β, as n_d is not a monotonic function of β; nevertheless, simple calculations show that the magnitude of n_d increases for $\beta \in (0, 1/\omega_r)$ and decreases otherwise.

The above discussion showed that the point of interest for the drilling system is unstable due to the apparent negative damping effect. The primary goal of employing a controller for this system is to reverse this situation, i.e., rendering the operating point asymptotically stable. The control technique developed in the following section is based on the negative damping coefficient concept introduced, and aims to enlarge the limits of drill string safe operation by finding the control gains that maximize the value of the negative damping coefficient for which the operating point is asymptotically stable.

ROBUST CONTROLLER DESIGN

This section proposes a controller that aims to maximize the robustness of the closed-loop system. The underlying principle of the proposed control technique is the negative damping coefficient and its influence on the local stability of the drilling system. As discussed previously, the apparent negative damping effect resulting from the bit-rock interaction is the main factor causing instability of the operating point. Due to the dependence of the negative damping coefficient on the drilling parameters indicated in Eq. (16), a controller that guarantees stability for a wide range of values of this coefficient will consequently allow stable drilling for a wide range of operating conditions (WOB and target angular velocity) and uncertainties in the friction parameters. To enlarge the region of safe drilling as much as possible, the proposed control technique aims to maximize the range of values of the negative damping coefficient for which the operating point is asymptotically stable. This idea can be formalized in the following manner.

Initially, aiming at the feasibility of controllers implementation, a simple control law with output feedback and static gain is considered

$$\begin{aligned} u &= -\mathbf{K}\mathbf{y} \\ \mathbf{y} &= \mathbf{C}\boldsymbol{\zeta} \end{aligned}. \tag{17}$$

Regarding measurements, two sensors were considered, with the output matrix given by

$$\mathbf{C} = \begin{bmatrix} 1 & 0 & 0 & 0 \\ \mathbf{0} & \bar{\boldsymbol{\phi}}(\alpha_1) - \bar{\boldsymbol{\phi}}(\alpha_2) & \mathbf{0} & \mathbf{0} \\ \mathbf{0} & \mathbf{0} & \boldsymbol{\phi}(\alpha_1) & \boldsymbol{\phi}(\alpha_2) \end{bmatrix}^{\intercal}, \tag{18}$$

in which α_1 and α_2 are the locations of the first and second sensors, respectively. Due to the need for an integrator at the rotary table, because the error derivative was defined as the difference between the rotary table and target velocities, the first sensor location is $\alpha_1 = 0$. Since sensors placement in field operations is limited, the second sensor was positioned at 10% of the total drill string length $\alpha_2 = 0.1L$. The first column of matrix $\mathbf{C}^{\intercal}$ corresponds to the error integral, the second is associated with the difference between the measured displacements, the third corresponds to the velocity measured at the rotary table and the fourth to the velocity measured at α_2.

For the control gain design, suppose the parameters of the friction function (1) are unknown and let $n_d \in \mathbb{R}_-$ represent a possible value that the negative damping coefficient may assume. Thus, the linearized closed-loop state matrix can be written as a function of the control gain $\mathbf{K}$ and n_d as

$$\mathbf{A}_{cl}(\mathbf{K}, n_d) = \mathbf{A}_{ln}(n_d) - \mathbf{B}_{tn}\mathbf{K}\mathbf{C}, \tag{19}$$

in which

$$\mathbf{A}_{ln} = \left.\frac{\partial \mathbf{h}}{\partial \boldsymbol{\zeta}}\right|_{\boldsymbol{\zeta}=\mathbf{0}}. \tag{20}$$

Next, for a given $\mathbf{K}$, define Z as the set of values of n_d for which the spectral abscissa of the linearized closed-loop state matrix $\nu(\mathbf{A}_{cl})$ is positive

$$Z = \{n_d \in \mathbb{R}_- \,|\, \nu(\mathbf{A}_{cl}(\mathbf{K}, n_d)) > 0\} \tag{21}$$

and γ as the supremum of this set

$$\gamma = \sup Z. \tag{22}$$

Then, the control gain is given by the optimization

$$\min_{\mathbf{K}} \ \gamma, \tag{23}$$

which aims to find the controller that guarantees asymptotic stability for the largest possible connected set of values of the negative damping coefficient. Since the negative damping coefficient is a monotonic function of several drilling parameters (WOB, ω_r, a_2, a_1), optimization (23) consequently guarantees asymptotic stability for the largest possible set of operating conditions (WOB and target angular velocity) and friction parameters.

NUMERICAL RESULTS

The effectiveness of the proposed control strategy is illustrated in this section by applying it to the model given in Eq. (13). Initially, the control gain was determined by performing optimization (23) using the SQP algorithm with several initial guesses and selecting the best local optimum. The optimum solution obtained was the control gain $\mathbf{K} = [0 \ -1990.8 \ 1071.0 \ -186.0]$, which yielded the cost function $\gamma = -542.3$ Nms. Note that the first component of the control gain is null, meaning that the controller that ensures asymptotic stability for the widest possible range of values of n_d has no integral action. However, due to the uncertainties involved in the drilling process, a controller without integral gain k_i would definitely generate a steady-state error. Thus, aiming to implement a controller with non-zero integral action, the influence of the integral gain on γ was analyzed by varying the first component of $\mathbf{K}$ while keeping the remaining control gains constant. The result of this analysis is indicated in Figure 2, which attests that γ assumes the lowest possible value for $k_i = 0$, and indicates that the closed-loop system robustness decreases monotonically as k_i increases. Therefore, considering only the steady-state error and robustness, a sensible decision would be to select the

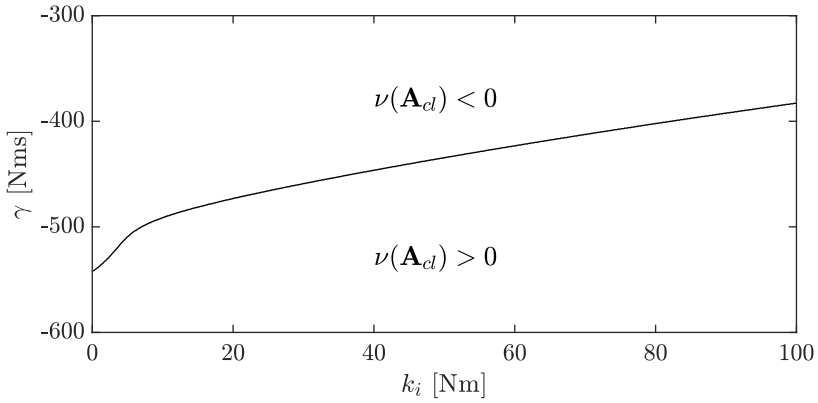

Figure 2 – Influence of the integral gain on γ.

smallest possible value of $k_i > 0$. However, the integral gain also plays a role in settling time, overshoot and stick phase duration.

To illustrate the influence of the integral gain on these aspects, simulations were performed using two values of this control gain: $k_i = 10$ and $k_i = 50$. The selected operating condition was a WOB of 160 kN and a target velocity of 100 rpm, and the initial condition was given by the drill string undeformed rotating with an angular velocity of 70 rpm, which is henceforth referred to as standard initial condition. Figure 3 depicts the bit and rotary table velocities for the two distinct values of the integral gain. The stick time duration corresponding to $k_i = 50$ is 8.06 s, whereas for $k_i = 10$ this interval is 19.74 s, more than twice that obtained for the higher control gain. The settling time (5% of the steady-state value) also indicates a remarkable advantage for the higher integral gain: 30.41 s for $k_i = 50$ and 111.34 s for $k_i = 10$. The only aspect in favor of the lower integral gain is the overshoot, which reached 95.6% for $k_i = 10$ and 119.4% for $k_i = 50$. Therefore, to achieve a trade-off between these aspects and the robustness of the closed-loop system, an intermediate value of 40 was adopted for k_i, yielding the control gain $\mathbf{K} = [40.0 \ -1990.8 \ 1071.0 \ -186.0]$.

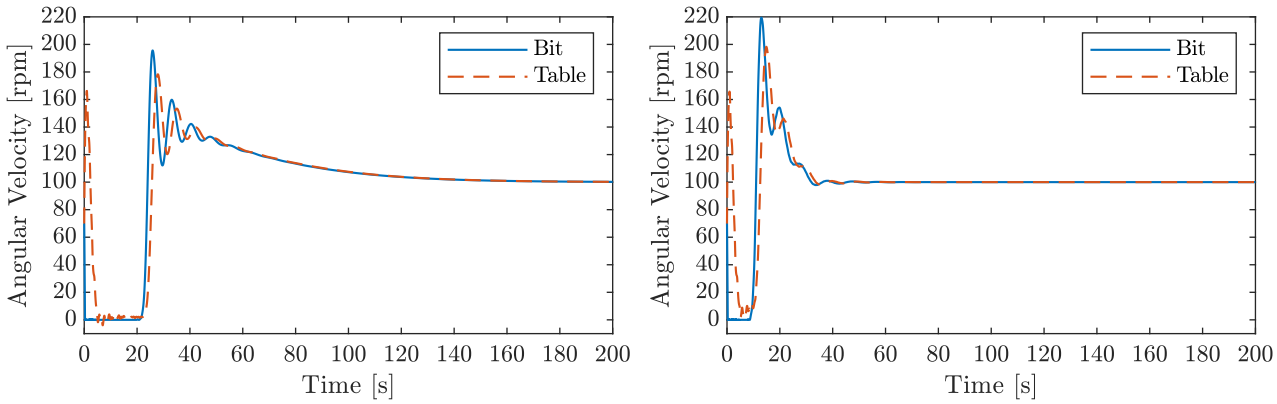

Figure 3 – Bit and rotary table velocities for $k_i = 10$ (left) and $k_i = 50$ (right) for WOB = 160 kN.

Although the control strategy developed provides maximum robustness for the closed-loop system regarding the negative damping coefficient, it gives no information about the nominal performance. To investigate how the proposed controller would perform in a nominal operating condition, its response is compared to that of a PI controller. The PI control gains were taken from Monteiro and Trindade (2017), who optimized the PI controller for a model very similar to the one adopted in the present paper. These control gains are $k_p = 675$ Nms and $k_i = 175$ Nm for the WOB of 120 kN, and $k_p = 650$ Nms and $k_i = 150$ Nm for the WOB of 140 kN. Figures 4 and 5 compare the response of the robust controller and both PI controllers. The general results for the simulations shown in these figures are given in Tab .3. According to these results, the robust controller performed better or equal to both PI controllers for all performance metrics considered. As discussed previously, it is still possible to improve the duration of the stick phase or settling time of the robust controller by increasing the integral gain, providing even better nominal results than the optimized PI controllers.

A final remarkable result of the robust controller concerns the stability of the operating point. The proposed methodology for the robust controller design relies on the spectral abscissa of the linearized closed-loop state matrix, thus ensuring asymptotic stability only for a neighborhood of the operating point. However, simulations with the nonlinear system suggest that the operating point is globally asymptotically stable for the region given by the intersection of the sets:

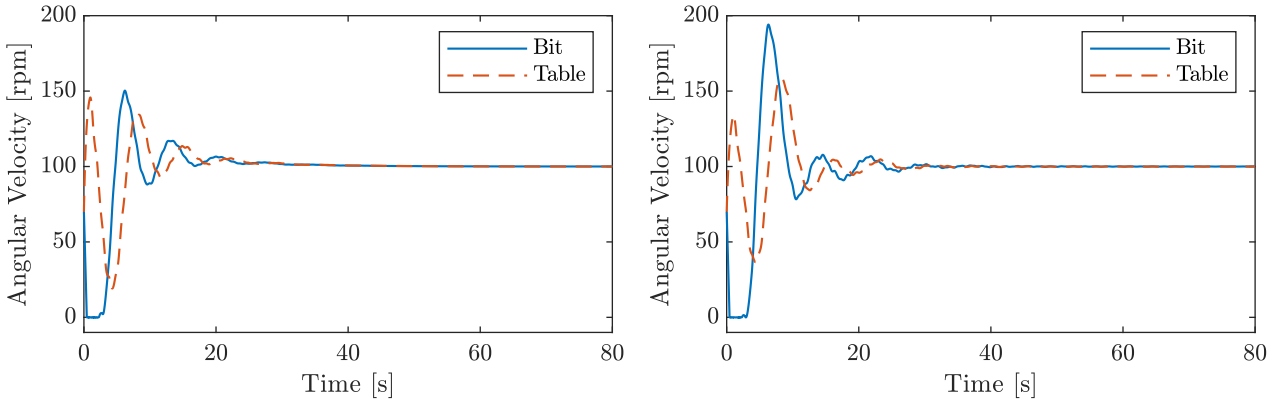

Figure 4 – Bit and rotary table velocities for Robust (left) and PI (right) controllers for WOB = 120 kN.

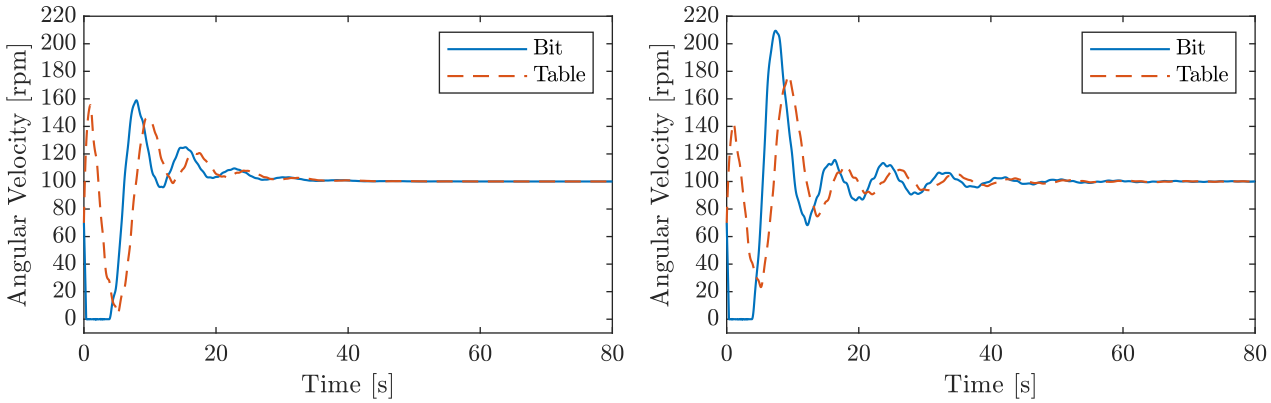

Figure 5 – Bit and rotary table velocities for Robust (left) and PI (right) controllers for WOB = 140 kN.

Table 3 – Main results for PI and Robust controllers.

WOB	Controller	Stick Time (s)	Overshoot (%)	Settling Time (s)
120 kN	PI	2.51	94.1	22.20
	Robust	1.80	50.3	21.45
140 kN	PI	3.49	109.4	34.00
	Robust	3.49	58.9	24.92

$$D = \{(k_i, n_d) \,|\, \nu(\mathbf{A}_c) < 0\}, \qquad E = \left\{(k_i, n_d) \,|\, 0 < k_i < \bar{k}_i\right\} \tag{24}$$

in which $\bar{k}_i = 69.6$. The region of the apparent global asymptotic stability of the operating point is highlighted in Fig. 6.

To illustrate the above statements, simulations were performed for the two points highlighted in Fig. 6 that are almost at the boundary of the stability region: $(k_i, n_d) = (15, -478)$ and $(k_i, n_d) = (69, -412)$. The friction curve that provided the desired negative damping coefficient in each case was selected from a variation of the friction coefficients a_1 and a_2 corresponding to the WOB of 160 kN. For example, the friction parameters corresponding to the WOB of 160 kN (Tab. 2) and a target velocity of 100 rpm result in a negative damping coefficient $n_d = -359.5$ Nms. To reach the value $n_d = -478$, the friction coefficients were changed to $a_1 = 0.020$ and $a_2 = 0.106$, keeping all other parameters constant. Note that the condition simulated for both points is harsher than the nominal one with the WOB of 160 kN, as the negative damping coefficient is lower in both cases. Figures 7 and 8 show the system response for both points considering two initial conditions: a small perturbation of the equilibrium point and the standard initial condition. Note that the system response always converge to the operating point regardless of the initial condition adopted. The simulation results also show the slow convergence of the response, as the eigenvalues in both cases are close to the imaginary axis. Similar results were obtained for every point in the region highlighted in Fig. 6 and for other initial conditions.

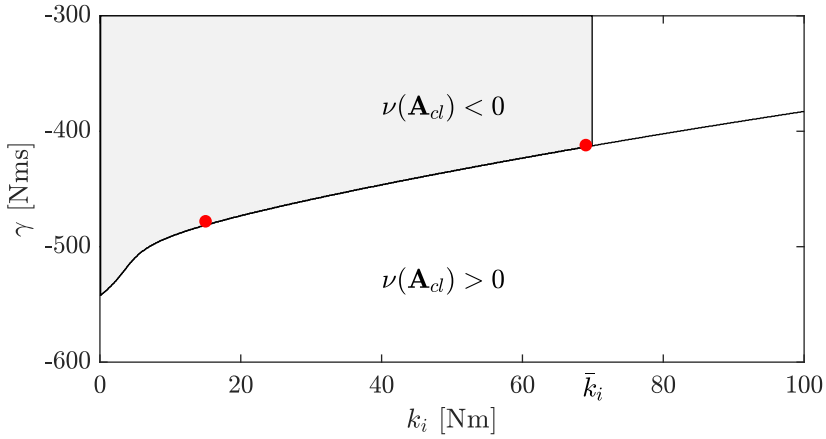

Figure 6 – Region of global stability of the operating point.

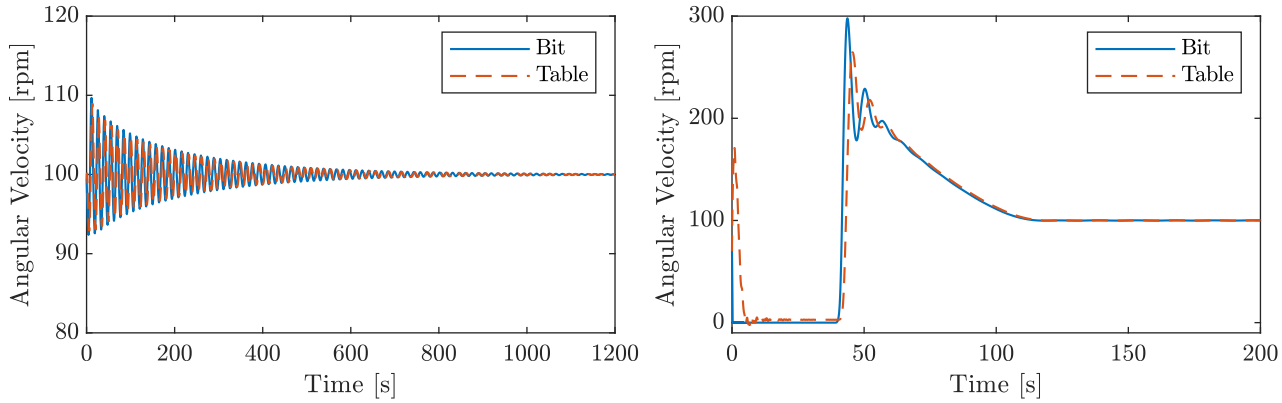

Figure 7 – Bit and rotary table velocities for two distinct initial conditions: a small perturbation of the equilibrium point (left) and the standard initial condition (right); $(k_i, n_d) = (15, -478)$**.**

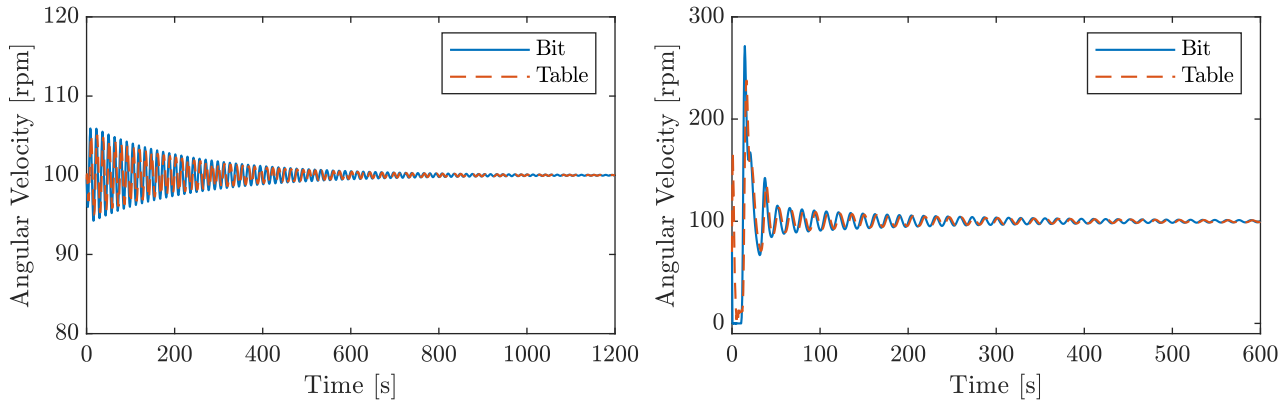

Figure 8 – Bit and rotary table velocities for two distinct initial conditions: a small perturbation of the equilibrium point (left) and the standard initial condition (right); $(k_i, n_d) = (69, -412)$**.**

CONCLUSIONS

This work has presented a novel methodology for controlling oil-well drill strings based on the concept of the negative damping coefficient. The introduction of the negative damping coefficient concept allowed key developments in the understanding of drill string dynamics and in the design of control laws:

- The negative damping coefficient explains experimental observations showing that increasing the WOB or decreasing the target angular velocity leads to stick-slip oscillations, and gives further information about the influence of other friction parameters on stability;

- The proposed control strategy provides remarkable robustness regarding parameter variations, while still maintaining good nominal performance;
- Although the controller design formulation employs the linearized system, simulations suggest there is a wide range of control gains values for which the operating point is globally asymptotically stable.

Results motivate further research in the investigation of the apparent global stability provided by the proposed controller and in the application of the proposed strategy for similar systems (Lure's problem).

ACKNOWLEDGMENTS

Financial support of the Coordination for the Improvement of Higher Education Personal (CAPES), Finance Code 001, and the National Council for Scientific and Technological Development (CNPq), grants 309193/2014-1 and 309001/2018-8, is acknowledged.

REFERENCES

Abdulgalil, F. and Siguerdidjane, H., 2004. "Nonlinear control design for suppressing stick-slip oscillations in oil well drillstrings". In *2004 5th Asian Control Conference (IEEE Cat. No.04EX904)*. Vol. 2, pp. 1276–1281.

Andronov, A.A., Vitt, A. and Khaikin, S.E., 1966. *Theory of Oscillators (translated from Russian)*. Pergamon Press, Oxford.

Brett, J., 1992. "The genesis of torsional drillstring vibrations". *SPE DRILLING ENGINEERING*, Vol. 7, No. 3, p. 168 – 174.

Dong, G.J. and Chen, P., 2016. "A review of the evaluation, control, and application technologies for drill string vibrations and shocks in oil and gas well". *Shock and Vibration*.

Guckenheimer, J. and Holmes, P., 1983. *Nonlinear oscillations, dynamical systems, and bifurcations of vector fields*. Springer-Verlag, New York.

Jardine, S., Malone, D. and Sheppard, M., 1994. "Putting a damper on drillings bad vibrations". *Oilfield Review*, Vol. 6, No. 1, pp. 15–20.

Khalil, H., 2002. *Nonlinear Systems*. Prentice Hall.

Mihajlović, N., Van Veggel, A., Van De Wouw, N. and Nijmeijer, H., 2004. "Analysis of friction-induced limit cycling in an experimental drill-string system". *Journal of Dynamic Systems, Measurement and Control, Transactions of the ASME*, Vol. 126, No. 4, p. 709 – 720.

Monteiro, H.L.S. and Trindade, M.A., 2017. "Performance analysis of proportional-integral feedback control for the reduction of stick-slip-induced torsional vibrations in oil well drillstrings". *Journal of Sound and Vibration*, Vol. 398, pp. 28–38.

Saldivar, B., Mondié, S., Loiseau, J.J. and Rasvan, V., 2013. "Suppressing axial-torsional coupled vibrations in drillstrings". *Control Engineering and Applied Informatics*, Vol. 15, No. 1, pp. 3–10.

Tucker, R.W. and Wang, C., 2003. "Torsional vibration control and cosserat dynamics of a drill-rig assembly". *Meccanica*, Vol. 38, No. 1, pp. 143–159.

Vaziri, V., Oladunjoye, I.O., Kapitaniak, M., Aphale, S.S. and Wiercigroch, M., 2020. "Parametric analysis of a sliding-mode controller to suppress drill-string stick-slip vibration". *Meccanica*, Vol. 55, No. 12, pp. 2475–2492.

Vromen, T., van de Wouw, N., Doris, A., Astrid, P. and Nijmeijer, H., 2017. "Nonlinear output-feedback control of torsional vibrations in drilling systems". *International Journal of Robust and Nonlinear Control*, Vol. 27, No. 17, p. 3659 – 3684.

Zhu, X., Tang, L. and Yang, Q., 2014. "A literature review of approaches for stick-slip vibration suppression in oilwell drillstring". *Advances in Mechanical Engineering*, Vol. 2014.

RESPONSIBILITY NOTICE

The authors are the only responsible for the printed material included in this paper.